Current Optics and Photonics
Vol. 4, No. 4, August 2020, pp. 310-316

ISSN: 2508-7266(Print) / ISSN: 2508-7274(Online)
DOI: https://doi.org/10.3807/COPP.2020.4.4.310

Microwave Signal Spectrum Broadening System Based on Time Compression

Menglong Kong, Zhongwei Tan*, Hui Niu, Hongbo Li, and Hongpei Gao

Institute of Lightwave Technology, Key Lab of All Optical Network & Advanced Telecommunication Network, Ministry of Education, Beijing Jiaotong University, Beijing 100044, China

(Received March 3, 2020 : revised May 23, 2020 : accepted June 16, 2020)

We propose and experimentally demonstrate an all-optical radio frequency (RF) spectrum broadening system based on time compression. By utilizing the procedure of dispersion compensation values, the frequency domain is broadened by compressing the linear chirp optical pulse which has been multiplexed by the radio frequency. A detailed mathematical description elucidates that the time compression is a very preferred scheme for spectrum broadening. We also report experimental results to prove this method, magnification factor at 2.7, 8 and 11 have been tested with different dispersion values of fiber, the experimental results agree well with the theoretical results. The proposed system is flexible and the magnification factor is determined by the dispersion values, the proposed scheme is a linear system. In addition, the influence of key parameters, for instance optical bandwidth and the sideband suppression ratio (SSR), are discussed. Magnification factor 11 of the proposed system is demonstrated.

Keywords : Time compression, Spectrum broadening, Spectrum analysis
OCIS codes : (070.1170) Analog optical signal processing; (070.4790) Spectrum analysis; (070.6020) Continuous optical signal processing

I. INTRODUCTION

Time-stretch and time-lens have drawn significant interest in applications for various optical information processing techniques by utilizing the characteristics of dispersion broadening [1, 2]. One of applications in the time-stretch is to convert the high-speed signal into a low-speed signal, thereby weakening the effect of electronic bottleneck [3, 4]. The time-lens can be used to achieve Fourier transformation, spectral magnification [5], ultra-fast real-time broadband radio frequency analyzer [6] or used to develop an ultra-narrow optical pulse generator. For the reverse processing of time-stretch, the research on compressing the pulse modulated by a microwave drive signal can be used to achieve frequency-magnification. High-frequency pulsed microwave signals have found important applications such as in radar systems [7] and microwave tomography [8]. In 2009, a time domain telescopic system capable of compressing waveforms by a factor of 27 with a maximum compressed waveform bandwidth of greater than 270 GHz has demonstrated by Foster *et al*. [9]. The main method to generate a high-frequency microwave pulse is to multiply the carrier frequency of a low-frequency microwave drive signal [10]. A microwave spectrum analyzer system has been proposed and demonstrated in [11], The approach is reverse processing of time-stretch. However, this maximum broaden-frequency is limited by dispersion-induced power penalty when the modulator is in double-sideband (DSB) modulation.

In this paper, we propose and experimentally demonstrate a novel frequency magnification using single sideband (SSB) modulation based on time compression through dispersion compensation. The technique is implemented using two spans of dispersive fiber and a modulator. The proposed system has a similar setup to time-stretch, the difference is that the values of dispersion are not identical in magnitude in the time compression system. The analysis shows that broaden-frequency is limited by the dispersion-induced power penalty in double sideband (DSB) while the penalty can be eliminated in SSB modulation. The proposed

*Corresponding author: zhwtan@bjtu.edu.cn, ORCID 0000-0002-8916-1614
Color versions of one or more of the figures in this paper are available online.

system is flexible and the magnification factor is determined by the dispersion values, the time-aperture in time compression system can be almost as large as the period of the optical pulses, additionally, we also verified that the proposed scheme is a linear system. Potential applications of the magnification system include single-shot, ultrafast spectrum with high-resolution, spectral characterization of molecular transitions and transient and nonequilibrium behavior [5, 12-15].

II. METHODS

Figure 1 shows the detailed depiction of the time compression scheme.

Our system consists of two spans of fiber and a Mach-Zehnder modulator (MZM) illustrated in Fig. 1. The temporal and frequency counterpart are shown in Fig. 1(b). The frequency waveforms in Fig. 1(b) are not the optical spectra, but the Fourier transform of their temporal waveforms. It is assumed the values of the third-order dispersion (TOD) of the two spans of fiber are small and negligible, and only the group velocity dispersion (GVD) β_2 is considered.

Firstly, the performance of time compression system is analyzed when the modulator is in SSB modulation. It is assumed that the pulse generated by mode-locked laser (MLL) is a short transform-limited Gaussian pulse given by $E_1(\omega)=E_0\left(2\pi T_0^2\right)^{1/2}\exp\left(-\omega^2T_0^2/2\right)$, where T_0 is the pulse half-width and E_0 is the pulse amplitude. This Gaussian pulse is sent to the first single-mode fiber (SMF) and broadened to chirped-pulse. The SMF can be characterized by the transfer functions given by $G_1(\omega)=\exp\left(j\beta_2\omega^2L_1/2\right)$. After propagating through the first spool of fiber, the field becomes

$$E_2(\omega)=E_1(\omega)\exp\left(\frac{j\beta_2\omega^2L_1}{2}\right), \tag{1}$$

where L_1 is the length of the first fiber. The chirped-pulse is then directed into the MZM and modulated by an RF signal. To simplify the operation, only the group velocity dispersion is considered since the influence mainly originates from the dispersion β_2. If the modulating signal applied to the MZM is a sinusoidal signal of angular frequency ω_{RF}, under the small-signal-modulation condition, using Bessel functions, the field can be described as

$$\begin{aligned}E_3(t)&=\frac{1}{2}E_2(t)\left\{\exp\left[j\left(\frac{\pi}{2}+\frac{m}{2}\cos(\omega_{RF}t)\right)\right]+\exp\left(j\frac{m}{2}\sin(\omega_{RF}t)\right)\right\}\\&=\frac{1}{2}E_2(t)\sum_{n=-\infty}^{\infty}\left[\left(1+j^{n+1}\right)J_n\left(\frac{m}{2}\right)\exp\left(jn\omega_{RF}t\right)\right],\end{aligned} \tag{2}$$

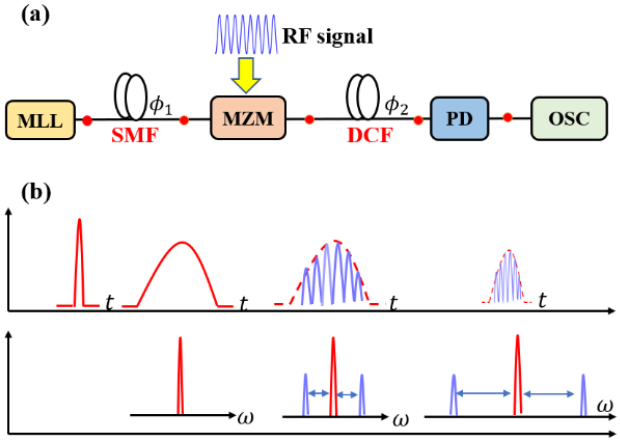

FIG. 1. (a) The structure of the time compression scheme. (b) Time domain and frequency domain process of the proposed system.

where $E_2(t)$ is time domains of the chirped-pulse. In addition, m is the modulation index defined as $m=\pi V_{RF}/V_\pi$, V_{RF} and V_π are the RF voltage amplitude and the half-wave voltage, respectively. Using the same derivation method as DSB modulation, this modulated waveform is compressed in the time domain through dispersion compensation fiber (DCF) which can be characterized by the transfer functions given by $G_2(\omega)=\exp\left(-j\beta_2\omega^2L_2/2\right)$. Finally, the broadened-frequency can be directly captured by the photodetector (PD) or spectrum analyzer. The photocurrent at the output of the PD is proportional to the intensity of the input electrical field, in the SSB modulation system, which is given by

$$I(t)\propto\left[1-\frac{m}{\sqrt{2}}\cos\left(\frac{\omega_{RF}}{M}t-\phi_{DIP}+\frac{\pi}{4}\right)+\exp\left(j\frac{m}{2}\sin\omega_{RF}t\right)\right], \tag{3}$$

where $\phi_{DIP}=(-\beta_2L_2\omega_{RF}^2)/2M$, L_2 is the length of the second fiber, $M=1-\Phi_2/\Phi_1$, $\Phi_1=\beta_2L_1$, $\Phi_2=\beta_2L_2$. In the proposed compression system, the dispersion values should satisfy $|\Phi_1|\neq|-\Phi_2|$ to make sure spectrum broadening. In addition, the dispersion-induced phase (DIP) is the most noteworthy factor that we can present linear dispersion, and it will result in a frequency-dependent attenuation as well as frequency-dependent harmonic distortion in the time compressed system. From the second term in the Eq. (3), an ideal frequency-magnification can be observed when the $\Phi_2<\Phi_1$, in other words, the spectrum of the RF signal is broadened. Therefore, the magnification factor is defined as 1/M. The key significance of the approach is that the magnification factor can be flexibly tunable by changing the dispersion values of the fiber.

In the DSB modulation, the coefficient of the second term includes the DIP, leading to frequency-dependent attenuation for output waveform. Additionally, the frequency-

dependent attenuation is periodic which originates from the intermodulation between the beating of carrier with the upper and the lower sidebands [2]. As can be seen from Eq. (3), DIP has been eliminated in the coefficient. However, it appears in the phase in the second term. Compared with the DSB modulation, it is indicated that there is no dispersion-induced phase which means that the attenuation introduced by the first-order dispersion can be removed by using SSB modulation. In the context of TS-ADC (Time-Stretched Analog-to-Digital Converter), the phase distortion could be removed in the digital domain using the known dispersion behavior of the fiber [2]. Therefore, the application of the SSB modulation will mainly depend on the digital error correction capability of phase interference.

III. SIMULATION

As discussed above, the simulation of time compression system is analyzed using Optisystem. The way to achieve SSB is as follows: The microwave voltage amplitudes of the upper and lower arms of the MZM are equal, a 90-degree phase shifter is used in the lower arm, the bias voltage is half of $V_{bias\pi}$, where $V_{bias\pi}$ is the half-wave voltage of bias. The chirped-pulse produced by the dispersion of the SMF should be optimized to satisfy the condition for which ω_{opt} is much larger than the ω_{RF}, where the ω_{opt} is optical bandwidth, as will be seen in the following simulation analysis. Gaussian pulse with a repetition rate of 100 MHz before the first l fiber L_1 is injected with bandwidth 3 THz compared with RF frequency 4 GHz. According to the definition of 1/M, it is assumed that the L_1 is 60 km and L_2 is 54 km and the SMF with dispersion of 1021 ps/nm and the DCF with dispersion of -918.9 ps/nm. Theoretically, the magnification factor is 10. MZM and sinusoidal signal are used to implement the intensity modulation.

Figure 2(a) shows the output waveform of the modulation, Fig. 2(b) shows the temporal domain after time compression system. It is indicated that the temporal domain of the RF signal is contained in the temporal domain envelope of the Gaussian pulse by measuring the time difference which is 0.025 ns between the two peaks. Figure 2 shows that the prediction of time-compression system design is proved. Simultaneously, higher-order harmonics accompanied by fundamental spectrum is observed. However, the power difference between the high-order harmonics and the fundamental spectrum is nearly 30 dB, which meets the requirements of the experiment.

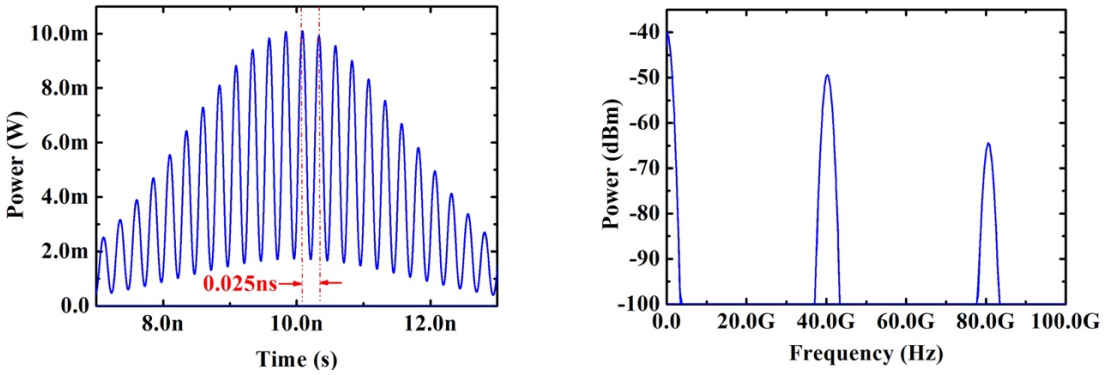

FIG. 2. (a) The time domain and (b) the frequency domain after time compression system.

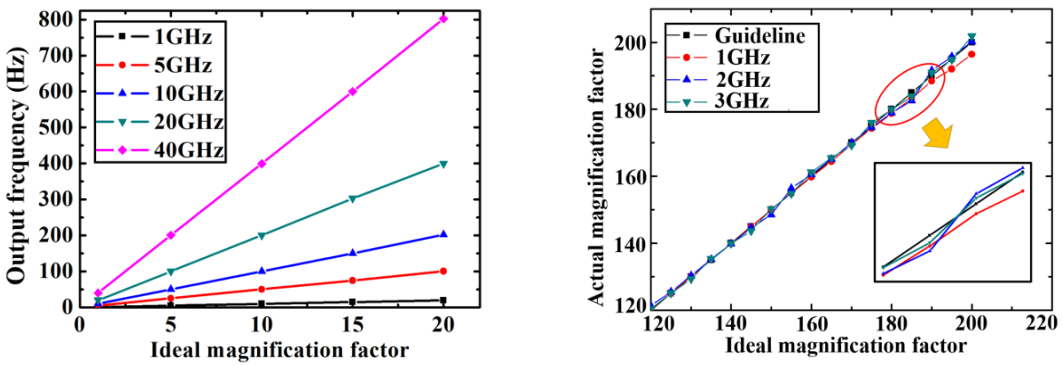

FIG. 3. The relationship between the ideal magnification factor and (a) output frequency, (b) actual magnification.

To investigate the performance of the scheme, we show the actual magnification in the time-compression system. By changing the length of the fiber, the magnification factor can be obtained while the output magnification frequency is observed through the RF spectrum analyzer. According to the simulation, Fig. 3(a) shows that the output frequency shows linear growth with tiny deviations compared with ideal frequency when the magnification factor is increasing. Figure 3(b) shows the actual magnification when the RF signal is 1 GHz, 2 GHz and 3 GHz while the magnification factor is from 120 to 200 (where the black trace is ideal magnification factor). Results show that the actual magnification has a small deviation compared with ideal magnification factor without considering the non-linearity. The inset shows the zoom-in fringes. It is indicated that our scheme is a linear system between ideal magnification factor and actual magnification which is beneficial for practical applications.

IV. EXPERIMENTS

Figure 4 shows the detailed depiction of the experimental setup.

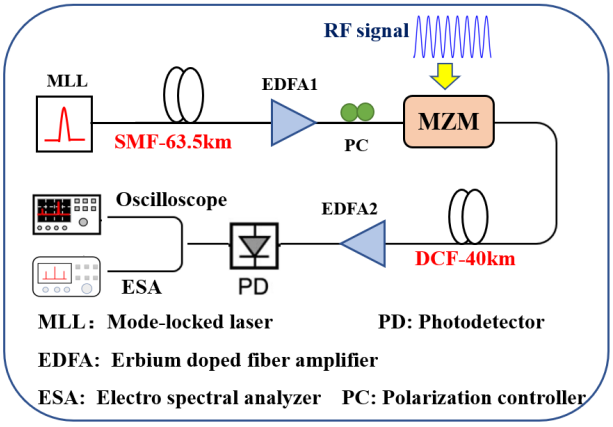

FIG. 4. The principle of detailed experimental setup.

The mode-locked laser, applied for the pulse sources with 1.5 ps pulse width and 50 MHz repetition rate, is used. In order to generate chirped-pulse, the Gaussian pulse wave centered at 1565 nm is spectrally isolated and sent through 63.5 km of SMF, broadening the pulse from 1.5 ps to 6 ns. Then, the RF signal is multiplexed onto the chirped-pulse through an intensity modulator. Subsequently, the modulator is followed with DCF which is 40 km and chosen to satisfy the dispersion of L_1, yielding the compressed waveform. Two amplifiers are used, one is before the modulator and the other is followed the DCF to compensate for power attenuation. According to the parameters of the L_1 and L_2, the spectrum magnification factor is 2.7. Finally, the compressed waveform is captured by a 40 GHz PD, a 50 GHz synchronous oscilloscope and an ESA with 28 GHz bandwidth.

We assume the sinusoidal modulating signal has a frequency of 1 GHz, Fig. 5(a) shows the output of temporal domain. The blue trace is the compressed waveform, with the mark as the zoom-in observation to show the magnification factor. Figure 5(b) shows that the output spectrum is at 2.7 GHz presented in the ESA. The experimental results agree well with the theoretical results.

The frequency resolution and the spectral range of the time compressed system are mainly determined by the dispersion of the fiber. As shown in the Fig. 5. Signal-to-noise ratio can be increased by increasing power and the length of fiber of the system is a certain deviation. The noise of the output spectrum is due to the fact that the measured signal power is close to the sensitivity of the system and the duty cycle of the compression system is small [2] and the distortions around the ideal broaden-frequency originates from instrument noise. In addition, there are some low frequency combs which are less than 1 GHz, it is generated by the 50 MHz repetition rate from MLL. The same phenomenon occurs around the 2.7 GHz when the system is tested in the time, the combs will not be observed within one optical pulse [16].

To verify the capability of the proposed system, magnification factors at 8 and 11 were also tested. The SMF with

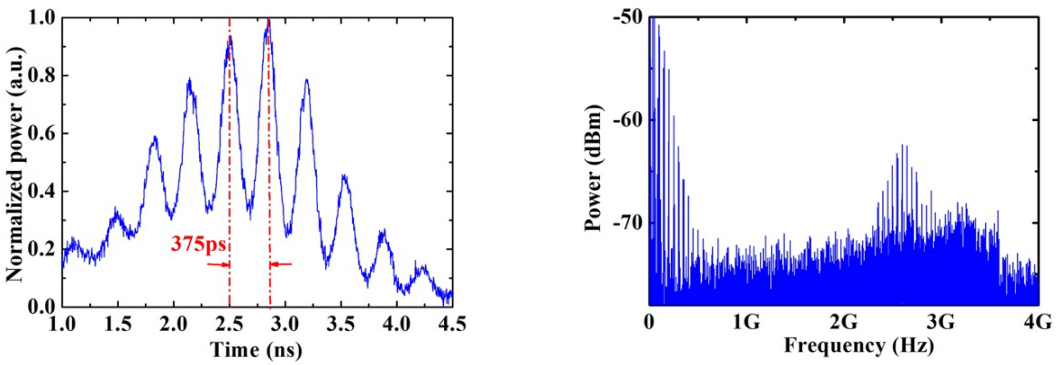

FIG. 5. The output of temporal domain (a) and the spectrum (b) with testing the frequency when magnification factor is 2.7.

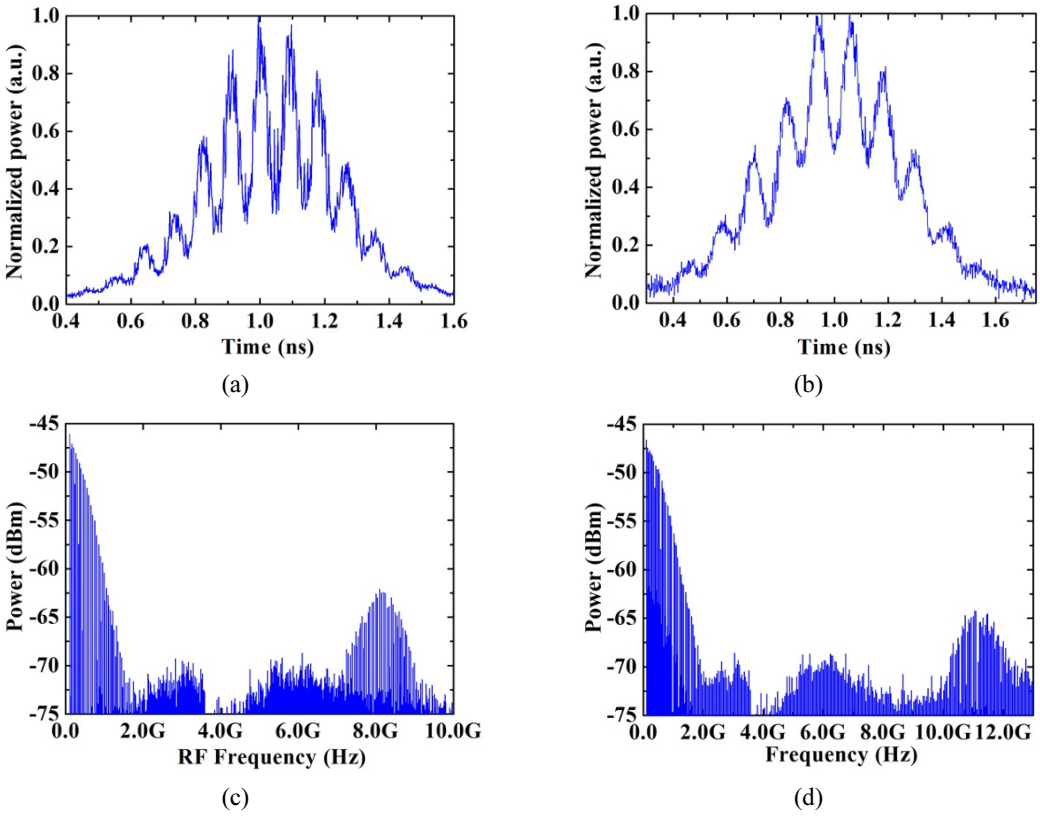

FIG. 6. The output in (a) temporal domain and (c) frequency domain when magnification factor is 8. The output in (b) temporal domain and (d) frequency domain when magnification factor is 11.

TABLE 1. Experimental parameters and results

D_1 (ps/nm)	D_2 (ps/nm)	*fin* (GHz)	*M*	*fout* (GHz) (theoretical)	*fout* (GHz) (measured)
1081.3	-681.12	1	2.7	2.7	2.66
1165.7	-1021.7	1	8	8	8.02
1122.4	-1021.7	1	11	11	11.01

dispersion of 1165.7 ps/nm and 1122.4 ps/nm, respectively, are to be used, and the dispersion of the DCF is changed to -1021.7 ps/nm. However, the increasing of the magnification factor will lead to increasing the loss and the signal-to-noise ratio of the output spectrum is reduced gradually as separately shown in Fig. 6. Figures 6(a) and 6(c) show the output of temporal domain and frequency domain when magnification factor is 8, Figs. 6(b) and 6(d) show the output of temporal domain and frequency domain when the magnification factor is 11. Besides that, high-order harmonics are also increasing. Note that the generated frequencies are relatively low, limited by the low operation bandwidth of the ESA.

The broaden-frequency are measured both in the time and frequency domains shown in Figs. 5 and 6. Experimental parameters and results are summarized in Table 1.

D_1 and D_2 are the dispersion value of the system, *fin* is the frequency applied on MZM, *fout* is the broaden-frequency.

V. DISCUSSION

In our analysis, it can be concluded that SSB modulation is the preferred modulation method. However, in practical considerations, the sideband of the signal during SSB modulation may not be completely removed and there will be a certain amplitude residual which will affect the performance of the SSB modulation system. Therefore, the sideband suppression ratio (SSR) is defined to describe the magnitude of the residual amplitude which represents the ratio of the amplitudes of the upper and lower sideband after modulation. Hence, the output form of temporal domain can be replaced as

$$E_3(t) = \frac{E_2(t)}{2}\left\{\exp\left[j\left(\frac{\pi}{2}+\frac{m}{2}\cos\omega_{RF}t\right)\right]+\exp\left[j\frac{rm}{2}\sin(\omega_{RF}t+\Delta\Phi\right]\right\}$$
$$= \frac{E_2(t)}{2}\sum_{n=-\infty}^{\infty}\left[J_n\left(\frac{m}{2}\right)j^{n+1}+J_n\left(\frac{rm}{2}\right)\exp(jn\Delta\Phi)\right]\exp(jn\omega_{RF}t), \quad (4)$$

where r is the inter-electrode signal amplitude ratio (ideally equal to unity) and $\Delta\phi$ is the deviation of inter-electrode

phase. The r and $\Delta\phi$ are mainly determined by the quality of the coupler and the symmetry between the two electrodes of the modulator. Therefore, the sideband suppression ratio is defined as R which is given by

$$R=\left|\frac{J_1(\frac{rm}{2})\exp(j\Delta\Phi)-J_1(\frac{m}{2})}{J_1(\frac{rm}{2})\exp(-j\Delta\Phi)+J_1(\frac{m}{2})}\right|\approx\left|\frac{r\exp(j\Delta\Phi)-1}{r\exp(j\Delta\Phi)+1}\right|. \quad (5)$$

The equation is established when m is very small. It demonstrates that the SSR is independent of m and relies on the phase and amplitude imbalance between the two arms. The photocurrent intensity of the PD is written as

$$I(t)\propto\cos(\omega_{RF}t-\phi_{DIP})+R\cos(\omega_{RF}t+\phi_{DIP}). \quad (6)$$

As an example, when $R=1$, the Eq. (6) can be simplified to the situation of DSB modulation (integration and difference), the attenuation amplitude of the output waveform is $\cos^2\phi_{DIP}$. When $R=0$, the Eq. (6) can be written to the SSB modulation. Therefore, the amplitude attenuation due to dispersion can be described as

$$H(f_{RF})=\left(\frac{1-R}{1+R}\right)^2\sin^2(\phi_{DIP})+\cos^2(\phi_{DIP}). \quad (7)$$

Figure 7 depicts the power penalty for different SSR. It can be suggested from the figure, as the R decreases, the dispersion penalty can be reduced by using the SSB modulation even with an imperfect SSB modulation. In fact, which meets most applications.

Finally, in order to show the influences of optical pulse bandwidth ω_{opt}. T_0 (where $\omega_{opt}=1/T_0$) is considered which was neglected before. To simplify the analysis, the linear modulation and no higher order harmonic term are assumed for the modulator. the light intensity of PD can be expressed as

$$I(t)\propto\left[J_0^2\left(\frac{M}{2}\right)-2\sqrt{2}J_0\left(\frac{M}{2}\right)J_1\left(\frac{M}{2}\right)\times\left(\cos\left(\frac{\omega_{RF}}{M}t-\phi_{DIP}+\frac{\pi}{4}\right)+E_{rr}+\ldots\right)\right], \quad (8)$$

$$E_{rr}=-\frac{\omega_{RF}\left(1-\frac{1}{M}\right)}{\omega_{opt}^2\beta_2(L_1-L_2)}t\cos\left(\frac{\omega_{RF}}{M}t-\phi_{DIP}+\frac{\pi}{4}\right). \quad (9)$$

E_{rr} is the interference of the output waveform. MATLAB is used to show interference model with various finite optical bandwidth. The output is also been separately reported with optical pulse bandwidth at 2 nm in Fig. 8(a) and 10 nm in Fig. 8(b). As illustrated, the amplitude-decreasing will be diminished, it is in an ideal situation where ω_{opt} is much larger than the ω_{RF}. Hence, in the experiments, the femtosecond laser with optical pulse bandwidth of up to 10 nm is demanded to be used aiming to reduce the interference.

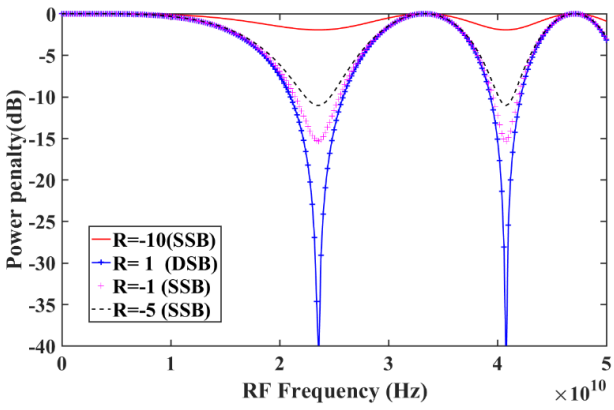

FIG. 7. Power penalty with the sideband suppression ratio decreasing.

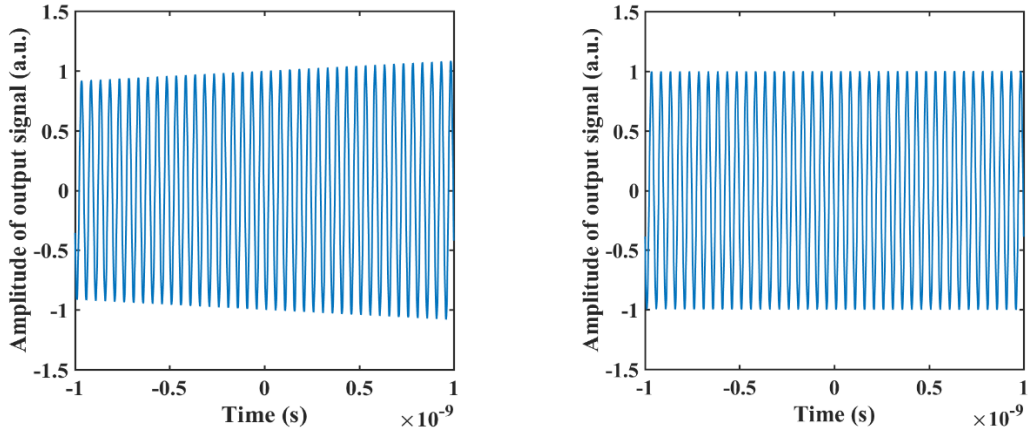

FIG. 8. Amplitude-decreasing caused by interference when (a) ω_{opt} = 2 nm and (b) ω_{opt} = 10 nm.

VI. CONCLUSION

In conclusion, a spectrum broadening system based on the time compression has been proposed and demonstrated. By analytical methods, it is shown that DIP can be eliminated in the SSB modulation. Simulation is done to show that the time compression system can be used in a very wide bandwidth and the spectrum of the signal can be broadened largely. Testing the frequency of the microwave signal at 1 GHz when the magnification factor is 2.7. Magnification factor at 8 and 11 were also tested with different dispersion values of fiber, the experimental results agree well with the theoretical results, it is indicated that the proposed scheme is a linear system. As the magnification factor increases, the signal-to-noise ratio gradually decreases which is due to the very small duty cycle of the optical pulses. Additionally, the attenuation of the output waveform amplitude can be reduced by using the SSB modulation with the R decreasing or the increasing optical pulse bandwidth.

ACKNOWLEDGMENT

This work is supported partially by the National Natural Science Foundation of China (Nos. 61875008).

REFERENCES

1. B. H. Kolner, "Space-time duality and the theory of temporal imaging," IEEE J. Quantum Electron. **30**, 1951-1963 (1994).
2. Y. Han and B. Jalali, "Photonic time-stretched analog-to-digital converter: fundamental concepts and practical considerations," J. Lightwave Technol. **21**, 3085-3103 (2003).
3. J. Wu, Y. Xu, J. Xu, X. Wei, A. C. Chan, A. H. Tang, A. K. Lau, B. M. Chung, H. C. Shum, E. Y. Lam, K. K. Wong, and K. K. Tsia, "Ultrafast laser-scanning time-stretch imaging at visible wavelengths," Light: Sci. Appl. **6**, e16196 (2017).
4. J. Ru, Q. Xie, C. Huang, B. Zheng, and C. Shu, "Enhanced performance in serial-to-parallel data conversion via Raman-assisted time lens processing," Opt. Lett. **42**, 1939-1942 (2017).
5. Y. Okawachi, R. Salem, M. A. Foster, A. C. Turner-Foster, M. Lipson, and A. L. Gaeta, "High-resolution spectroscopy using a frequency magnifier," Opt. Express **17**, 5691-5697 (2009).
6. L. Chen, Y. Duan, H. Zhou, X. Zhou, C. Zhang, and X. Zhang, "Real-time broadband radio frequency spectrum analyzer based on parametric spectro-temporal analyzer (pasta)," Opt. Express **25**, 9416-9425 (2017).
7. C. Wang and J. P. Yao, "Photonic generation of chirped millimeter-wave pulses based on nonlinear frequency-to-time mapping in a nonlinearly chirped fiber Bragg grating," IEEE Trans. Microwave Theory Tech. **56**, 542-553 (2008).
8. M. Bertero, M. Miyakawa, P. Boccacci, F. Conte, K. Orikasa, and M. Furutani, "Image restoration in chirp-pulse microwave CT (CP-MCT)," IEEE Trans. Biomed. Eng. **47**, 690-699 (2000).
9. M. A. Foster, R. Salem, Y. Okawachi, A. C. Turner-Foster, M. Lipson, and A. L. Gaeta, "Ultrafast waveform compression using a time-domain telescope," Nat. Photonics **3**, 581-585 (2009).
10. C. Wang, M. Li, and J. Yao, "Continuously tunable photonic microwave frequency multiplication by use of an unbalanced temporal pulse shaping system," IEEE Photonics Technol. Lett. **22**, 1285-1287 (2010).
11. R. E. Saperstein, D. Panasenko, and Y. Fainman, "Demonstration of a microwave spectrum analyzer based on time-domain optical processing in fiber," Opt. Lett. **29**, 501-503 (2004).
12. F. Vestin, K. Nilsson, and P.-E. Bengtsson, "Validation of a rotational coherent anti-Stokes Raman spectroscopy model for cabon dioxide using high-resolution detection in the temperature range 294-1143K," Appl. Opt. **47**, 1893-1901 (2008).
13. N. Qian, W. Zou, S. Zhang, and J. Chen, "Signal-to-noise ratio improvement of photonic time-stretch coherent radar enabling high-sensitivity ultrabroad W-band operation," Opt. Lett. **43**, 5869-5872 (2018).
14. B. Wang, P. Lu, S. J. Mihailov, X. Fan, and J. P. Yao, "Real-time and high-precision interrogation of a linearly chirped fiber Bragg grating sensor array based on dispersive time delay and optical pulse compression," Opt. Lett. **44**, 3246-3249 (2019).
15. Y. Tong, Q. Zhou, D. Han, B. Li, W. Xie, Z. Liu, J. Qin, X. Wang, Y. Dong, and W. Hu, "Photonic generation of phase-stable and wideband chirped microwave signals based on phase-locked dual optical frequency combs," Opt. Lett. **41**, 3787-3790 (2016).
16. L. K. Mouradian, F. Louradour, V. Messager, A. Barthelemy, and C. Froehly, "Spectro-temporal imaging of femtosecond events," IEEE J. Quantum Electron. **36**, 795-801 (2000).